Control of Hydrogen Photoproduction by the Proton Gradient Generated by Cyclic Electron Flow in Chlamydomonas reinhardtii [W]

Dimitri Tolleter,[a,b,c,1] Bart Ghysels,[a,b,c,1] Jean Alric,[d] Dimitris Petroutsos,[e] Irina Tolstygina,[e] Danuta Krawietz,[f] Thomas Happe,[f] Pascaline Auroy,[a,b,c] Jean-Marc Adriano,[a,b,c] Audrey Beyly,[a,b,c] Stéphan Cuiné,[a,b,c] Julie Plet,[a,b,c] Ilja M. Reiter,[b,c,g] Bernard Genty,[b,c,g] Laurent Cournac,[a,b,c] Michael Hippler,[e] and Gilles Peltier[a,b,c,2]

[a] Commissariat à l'Energie Atomique et aux Energies Alternatives, Direction des Sciences du Vivant, Institut de Biologie Environnementale et de Biotechnologie, Laboratoire de Bioénergétique et Biotechnologie des Bactéries et Microalgues, Commissariat à l'Energie Atomique Cadarache, 13108 Saint-Paul-lez-Durance, France

[b] Centre National de la Recherche Scientifique, Unité Mixte de Recherche 6191 Biologie Végétale et Microbiologie Environnementale, 13108 Saint-Paul-lez-Durance, France

[c] Aix Marseille Université, Unité Mixte de Recherche 6191 Biologie Végétale et Microbiologie Environnementale, 13108 Saint-Paul-lez-Durance, France

[d] Institut de Biologie Physico-Chimique, Unité Mixte de Recherche 7141, Centre National de la Recherche Scientifique, Université Pierre et Marie Curie-Paris 6, 75005 Paris, France

[e] Institute of Plant Biology and Biotechnology, University of Münster, 48143 Munster, Germany

[f] Ruhr University Bochum, Department of Biology and Biotechnology, AG Photobiotechnology, 44780 Bochum, Germany

[g] Commissariat à l'Energie Atomique et aux Energies Alternatives, Direction des Sciences du Vivant, Institut de Biologie Environnementale et de Biotechnologie, Laboratoire d'Ecophysiologie Moléculaire des Plantes, Commissariat à l'Energie Atomique Cadarache, 13108 Saint-Paul-lez-Durance, France

Hydrogen photoproduction by eukaryotic microalgae results from a connection between the photosynthetic electron transport chain and a plastidial hydrogenase. Algal H_2 production is a transitory phenomenon under most natural conditions, often viewed as a safety valve protecting the photosynthetic electron transport chain from overreduction. From the colony screening of an insertion mutant library of the unicellular green alga *Chlamydomonas reinhardtii* based on the analysis of dark-light chlorophyll fluorescence transients, we isolated a mutant impaired in cyclic electron flow around photosystem I (CEF) due to a defect in the Proton Gradient Regulation Like1 (PGRL1) protein. Under aerobiosis, nonphotochemical quenching of fluorescence (NPQ) is strongly decreased in *pgrl1*. Under anaerobiosis, H_2 photoproduction is strongly enhanced in the *pgrl1* mutant, both during short-term and long-term measurements (in conditions of sulfur deprivation). Based on the light dependence of NPQ and hydrogen production, as well as on the enhanced hydrogen production observed in the wild-type strain in the presence of the uncoupling agent carbonyl cyanide *p*-trifluoromethoxyphenylhydrazone, we conclude that the proton gradient generated by CEF provokes a strong inhibition of electron supply to the hydrogenase in the wild-type strain, which is released in the *pgrl1* mutant. Regulation of the *trans*-thylakoidal proton gradient by monitoring *pgrl1* expression opens new perspectives toward reprogramming the cellular metabolism of microalgae for enhanced H_2 production.

INTRODUCTION

A few microalgae species, including the model species *Chlamydomonas reinhardtii*, have been reported to produce H_2 in the light (Gaffron and Rubin, 1942; Healey, 1970). During this process, electrons produced by the photosynthetic electron transport chain are diverted at the level of ferredoxin toward [Fe-Fe] hydrogenase, which catalyzes the reversible reduction of protons into molecular hydrogen in algae (Florin et al., 2001). The use of microalgae is considered to be a promising approach for developing sustainable H_2 production from sunlight energy and water as the main resources (Melis and Happe, 2001). However, this mechanism represents a quantitatively minor and transitory phenomenon under most natural conditions and is often considered as a safety mechanism that would protect the photosynthetic apparatus from overreduction (Melis and Happe, 2001; Happe et al., 2002; Hemschemeier et al., 2009). Harnessing and enhancing microalgal H_2 production is recognized as a major step in developing clean and sustainable hydrogen economy (Ghirardi et al., 2000; Melis, 2002; Kruse et al., 2005a).

---

[1] These authors contributed equally to this work.

[2] Address correspondence to gilles.peltier@cea.fr.

The author responsible for distribution of materials integral to the findings presented in this article in accordance with the policy described in the Instructions for Authors (www.plantcell.org) is: Gilles Peltier (gilles.peltier@cea.fr).

[W] Online version contains Web-only data.

www.plantcell.org/cgi/doi/10.1105/tpc.111.086876

The main limitation to hydrogen production is considered to result from the O_2 sensitivity of hydrogenase enzymes: molecular O_2 produced at photosystem II (PSII) during photosynthesis rapidly induces the irreversible inhibition of the algal [FeFe]-hydrogenase (Happe et al., 2002; Stripp et al., 2009). An experimental protocol based on sulfur deficiency was reported to circumvent this limitation by inducing a time-based separation of O_2- and H_2-producing phases (Melis et al., 2000). During this process, the reducing power generated by photosynthesis is temporarily stored as starch during the aerobic phase and consumed during a subsequent anaerobic period to supply reductants either to produce H_2 or to maintain anaerobiosis by feeding mitochondrial respiration (Melis et al., 2000; Chochois et al., 2009). Other experimental approaches have used genetic engineering aiming at lowering the O_2 sensitivity of hydrogenase. Although such a strategy has proven its feasibility in bacterial [NiFe]-hydrogenases (Dementin et al., 2009), efficient engineering resulting in a decrease in the O_2 sensitivity of the microalgal [FeFe]-hydrogenase has not been yet reported. In addition to the hydrogenase O_2 sensitivity, optimization of the electron supply to the hydrogenase appears a critical issue. Two main pathways of electron supply have been previously identified under conditions of sulfur limitation, a direct and an indirect pathway (Fouchard et al., 2005; Chochois et al., 2009). During the direct pathway, hydrogen is produced using electrons supplied by the photosynthetic electron transport chain from PSII to photosystem I (PSI) and then to the hydrogenase via reduced ferredoxin. During the indirect pathway, the reducing power generated by oxygenic photosynthesis, first stored as starch in response to sulfur starvation, is remobilized in a second step. During this process, the reducing equivalents generated during starch catabolism are injected into the intersystem electron transport chain at the level of the plastoquinone (PQ) pool. The enzyme involved in this process has recently been identified as a plastidial type II NADH dehydrogenase called Nda2 (Jans et al., 2008; Desplats et al., 2009). Both pathways of hydrogen production share common electron carriers, such as the cytochrome b_6/f complex, plastocyanin, and PSI.

In addition to the linear electron flow of photosynthesis, cyclic electron flow (CEF) around PSI allows the recycling of electrons available on the acceptor side of PSI (reduced ferredoxin or NADPH) toward the intersystem electron transport chain, namely, the PQ pool or the cytochrome b_6/f complex. CEF has been shown to generate a thylakoid trans-membrane proton gradient involved in the establishment of nonphotochemical quenching (NPQ). In Chlamydomonas, CEF is regulated by state transition (Finazzi et al., 2002), a phenomenon involved in the redistribution of the excitation energy between PSI and PSII. Transition from state 1 to state 2 occurs in response to an increase in the redox state of the PQ pool, for instance, under anaerobic conditions. This triggers the STT7 kinase to phosphorylate mobile light-harvesting complex II (LHCII), resulting in a move of phosphorylated LHCII from PSII to PSI (Depège et al., 2003). CEF has been shown to be particularly active in state 2, where the existence of a functional supercomplex involved in CEF has been recently described. PGR5 was first identified in Arabidopsis thaliana as an essential molecular component of CEF from a screen of Arabidopsis mutants affected in NPQ (Munekage et al., 2002). More recently, Proton Gradient Regulation Like1 (PGRL1) has been identified in Arabidopsis as another essential component of CEF, interacting with both PGR5 and ferredoxin (DalCorso et al., 2008). In C. reinhardtii, downregulation of PGRL1 resulted in an impairment of CEF, particularly under conditions of iron deficiency (Petroutsos et al., 2009). Although a relationship between H_2 production and CEF has been proposed based on the study of a C. reinhardtii mutant affected in a nucleus-encoded mitochondrial protein (Kruse et al., 2005b), the mechanistic nature of this correlation remains to be established.

To identify new regulatory mechanisms of photosynthesis and explore novel strategies to improve H_2 production, we have set up a mutant screen based on the analysis of chlorophyll fluorescence transients in the unicellular green alga C. reinhardtii. The rationale of this approach was to consider that the photosynthetic electron transport is optimized to achieve optimal photosynthesis. We hypothesized that a perturbation in the regulatory process of photosynthesis could result in a redox imbalance that may lead to a stimulation of H_2 photoproduction. We report on the isolation of a mutant (pgrl1) affected in CEF around PSI and showing strongly increased hydrogen producing abilities. We conclude that the proton gradient generated by CEF around PSI strongly limits the electron supply to hydrogenase in wild-type algae.

RESULTS

A colony screen of a C. reinhardtii mutant library generated by the random insertion of a paromomycin resistance cassette (AphVIII) was performed under fully photoautotrophic growth conditions by recording chlorophyll fluorescence transients (Figures 1A and 1B). A dozen mutants differentially affected in chlorophyll fluorescence transients were isolated from the screen of 15,000 insertion strains. One of these mutants showed the absence of a transient fluorescence rise occurring in the 10- to 25-s range following the onset of illumination, indicating an alteration in the photosynthetic function (Figure 1B). This mutant harbored a unique insertion of the paromomycin resistance cassette in the PGRL1 gene (Figure 1C), resulting in the absence of PGRL1 transcript (Figure 1D) and protein (Figure 1E). Backcross of the mutant with a wild-type strain always showed cosegregation of antibiotic resistance and chlorophyll fluorescence properties. Chlorophyll fluorescence measurements were performed during a dark to light (75 μmol photons·m^{-2}·s^{-1}) transient on dark-adapted (30 min) cells in liquid cultures. Illumination with short saturating flashes allowed the determination of electron transport rate (ETR) activity and NPQ from chlorophyll fluorescence measurements shown in Supplemental Figure 1 online. Whereas the ETR was higher in the pgrl1 mutant than in the wild type (Figure 1F), NPQ remained lower (Figure 1G). The decrease in chlorophyll fluorescence (Fs) observed in the 10- to 30-s range in the pgrl1 mutant (Figure 1B; see Supplemental Figure 1 online); therefore, results from these two antagonistic effects (Figures 1F and 1G).

The ETR and NPQ were then determined as a function of light intensity in light-adapted cells (Figures 2D and 2E). The ETR
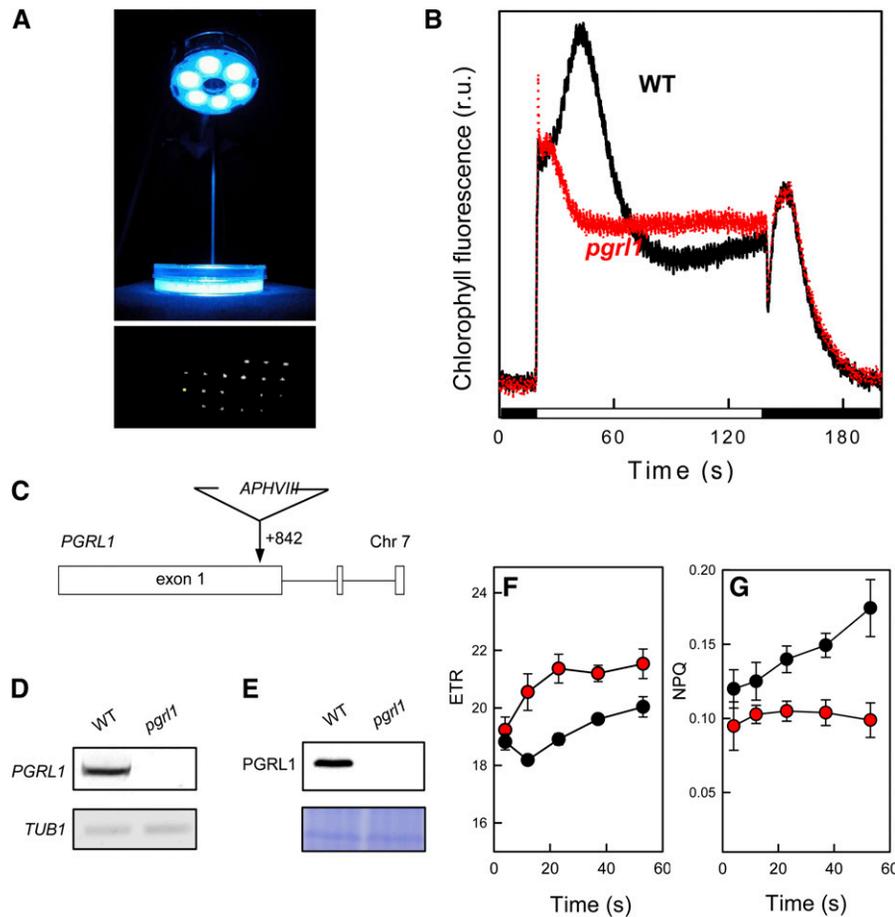
Figure 1. Isolation of the *pgrl1* Mutant from the Screening of a *Chlamydomonas* Insertion Mutant Library Based on the Analysis of Chlorophyll Fluorescence Transients.

(A) View of the experimental design used for colony screening of a *Chlamydomonas* insertion mutant library.

(B) Chlorophyll fluorescence transient recorded on a single colony during a dark–light–dark transient in wild-type cells and in a mutant (*pgrl1*) showing a modified fluorescence transient. The black and white boxes at the bottom indicate dark and light periods, respectively. r.u., relative units.

(C) Location of the insertion site of the *APHVIII* cassette conferring paromomycin resistance in chromosome 7, at the level of the first exon of the *PGRL1* gene.

(D) RT-PCR showing expression of *PGRL1* and *TUBULIN1* (*TUB1*) genes in the wild type (WT) and the *pgrl1* mutant.

(E) Immunoblot analysis of PGRL1 levels in the wild type and the *pgrl1* mutant (top panel) and loading control using Coomassie blue staining (bottom panel).

(F) and **(G)** Time course of ETR **(F)** and NPQ **(G)** determined from chlorophyll fluorescence measurements shown in Supplemental Figure 1 online during a dark–light transient. Actinic light (75 μmol photons·m^{-2}·s^{-1}) was switched on at T0 on 30 min dark-adapted *pgrl1* and wild-type cells. Data are expressed as average values $\pm$ SD (bars) of four independent experiments. Wild-type cells (black dots); *pgrl1* mutant cells (red dots).

reached similar values in *pgrl1* and in the wild type under a wide range of light intensities (Figure 2D). By contrast, NPQ was strongly diminished in *pgrl1* (Figure 2E). Strongly reduced NPQ ability was previously reported in *Arabidopsis* mutants affected in *PGR5* and *PGRL1* genes and was attributed to the existence of a lower light-induced proton gradient resulting from CEF impairment (Munekage et al., 2002; DalCorso et al., 2008). Activity of CEF was then measured by two different techniques: (1) reduction of PSI at 705 nm (Alric et al., 2010), and (2) relaxation of the electrochromic carotenoid bandshift (Joliot and Joliot, 2008), both methods being described in Supplemental Figure 2 online. These measurements clearly demonstrated a reduced activity of CEF in *pgrl1* when compared with the wild type. The effect was more pronounced under anaerobic conditions (Table 1), where CEF activity is increased due to a switch from state 1 to state 2 (Wollman and Delepelaire, 1984). In *C. reinhardtii*, LHCSR3, a stress-related member of the LHC protein superfamily, is required for the induction of the qE component of NPQ (Peers et al., 2009). As qE increases under high light, the amount of the LHCSR3 protein also increases under these growth conditions. To test whether the high light induction of the protein is functional in the PGRL1-deficient background, immunoblot analyses were conducted together with NPQ measurements in low light and high light acclimated cells (Figure 3). LHCSR3 amounts strongly
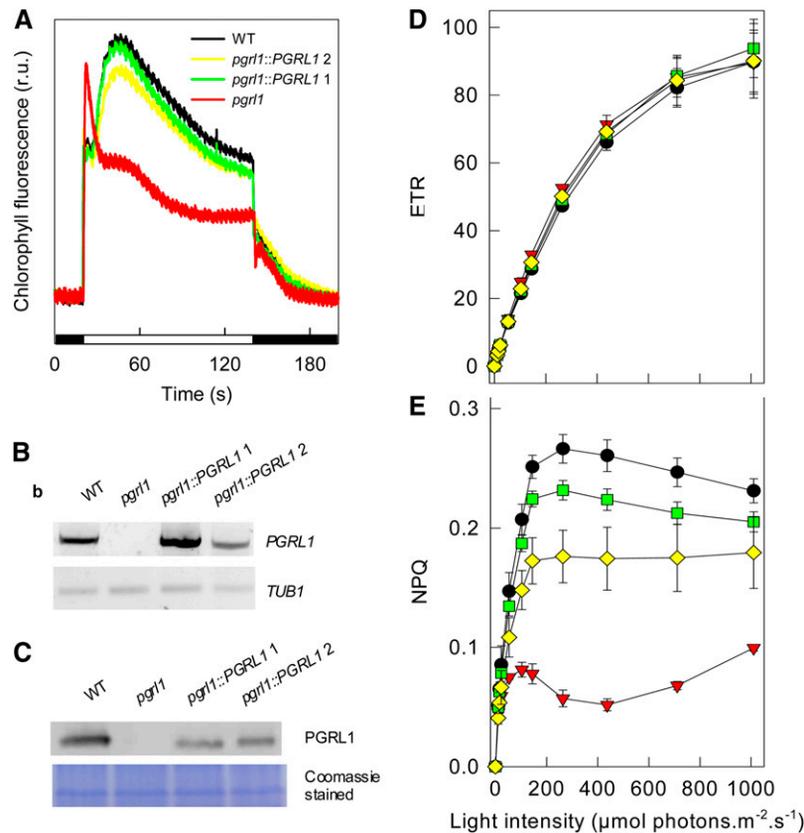
Figure 2. Complementation of the *pgrl1* Mutant and Light Dependence of ETR and NPQ.

Analysis of chlorophyll fluorescence properties and expression of PGRL1 transcript and protein in wild-type cells, in the *pgrl1* mutant, and in the two complemented lines *pgrl1::PGRL1* 1 and *pgrl1::PGRL1* 2.

(A) Chlorophyll fluorescence transient recorded on a single colony during a dark–light–dark transient in *C. reinhardtii* wild-type, in the *pgrl1* mutant, and in the two complemented strains *pgrl1::PGRL1* 1 and *pgrl1::PGRL1* 2. r.u., relative units.

(B) RT-PCR showing expression of *PGRL1* and *TUB1* genes. WT, wild type.

(C) Immunoblot analysis of PGRL1 (top panel) and loading control using Coomassie blue staining (bottom panel).

(D) and **(E)** ETR **(D)** and NPQ **(E)** determined from chlorophyll fluorescence measurements performed on light-adapted cells after 40 s of illumination at each given fluence. Data are expressed as average values ± SD (bars) of four independent experiments.

increased in response to high light both in *pgrl1* and in wild-type cells (Figure 3A). On the other hand, the NPQ increase observed in response to high light was much more pronounced in the wild-type than in the *pgrl1* mutant (Figures 3B and 3C). Therefore, in conditions of LHCSR3 induction, the decreased NPQ observed in the mutant does not result from a decrease in LHCSR3 amounts. We conclude from these experiments that, as in the *Arabidopsis pgr5* and *pgrl1* mutants, the decreased NPQ observed in the *Chlamydomonas pgrl1* mutant results from an impairment in CEF.

The *pgrl1* mutant was complemented by expressing a wild-type copy of the *PGRL1* gene under the control of its own promoter. Two strains, named *pgrl1::PGRL1* 1 and *pgrl1::PGRL1* 2, showed restoration of the chlorophyll fluorescence phenotype (Figure 2A) and expressed significant levels of the *PGRL1* transcript (Figure 2B) and protein (Figure 2C). The amount of PGRL1 protein present in *pgrl1::PGRL1* 1 and *pgrl1::PGRL1* 2 complemented strains was estimated to be around 50 to 60% of the

wild-type protein level. Chlorophyll fluorescence measurements and quenching analysis showed that NPQ was partly restored in *pgrl1::PGRL1* 2 and almost completely restored in *pgrl1::PGRL1* 1 (Figure 2E).

H$_2$ production capacities of the *pgrl1* mutant were then assayed using a membrane inlet mass spectrometer, which allows the measurement of gas exchange kinetics in cell suspensions (Cournac et al., 2002). Following dark anaerobic induction of hydrogenase, low light (50 μmol photons·m^{-2}·s^{-1}) was switched on, resulting in similar H$_2$ photoproduction in the wild type and in *pgrl1* (Figure 4A). At a higher light intensity (200 μmol photons·m^{-2}·s^{-1}), the rate of H$_2$ production rapidly decreased in the wild type, whereas in *pgrl1*, the initial H$_2$ production rate, which was similar to that measured in wild-type cells, was maintained at a high level during the light period (Figure 4C). This effect was fully reversed in the two complemented strains (Figure 4C). To determine to what extent the proton gradient generated by PGRL1-dependent CEF is involved in the limitation

**Table 1.** Measurements of CEF in the Wild Type and *pgrl1*

	Wild Type	*pgrl1*
CEF rate in electron s^{-1}·PSI^{-1} in aerobic conditions (from $\Delta A_{705 \text{ nm}}$)	37.1 ± 5.8	23.1 ± 1.3
Relaxation of electrochromic shift in aerobic conditions in (e$^-$·s^{-1}·PSI^{-1})	36.3 ± 1.6	23.3 ± 1.7
Relaxation of electrochromic shift in anaerobic conditions (e$^-$·s^{-1}·PSI^{-1})	46 ± 3.6	22 ± 2.1

CEF measurements were performed by following dark rereduction kinetics of flash-induced oxidized PSI at 705 nm or by following relaxation of the carotenoid electrochromic bandshift at 520 nm. Data are average values of three independent experiments ± SD.

of H$_2$ production observed in the wild type, we analyzed the effect of the uncoupling agent carbonyl cyanide *p*-trifluoromethoxyphenylhydrazone (FCCP). Whereas FCCP had a limited impact on H$_2$ production under low light conditions (Figure 4B), a strong increase in the H$_2$ production rate was observed upon FCCP addition under high light in the wild type and in the two complemented lines, with H$_2$ production reaching similar values in the mutant and wild-type strains (Figure 4D). We conclude from these experiments that the proton gradient generated by CEF severely restricts H$_2$ production under high light conditions in the wild type. Such a restriction does not occur in *pgrl1* due to a decrease in the proton gradient caused by CEF impairment, resulting in a higher light-dependent H$_2$ production rate.

Long-term capacities for H$_2$ production were then measured under conditions of sulfur deprivation, which is an efficient way to trigger and promote sustainable H$_2$ production (Melis et al., 2000). Among other effects, sulfur deprivation causes massive starch accumulation and a downregulation of PSII activity, which enables the establishment of long-term anoxia in the light (Melis et al., 2000). A strong (3- to 4-fold) increase in H$_2$ photoproduction capacity was observed in *pgrl1*, which was fully reversed in the two complemented lines (Figure 5). H$_2$ photoproduction rates was also increased (by ∼50%) in a *Chlamydomonas* RNA interference line expressing a lower level of PGRL1 (Petroutsos et al., 2009) (see Supplemental Figure 3 online). Two different pathways (direct and indirect) of H$_2$ production have been described. The direct pathway, which involves residual PSII activity feeding the photosynthetic electron transport chain, has been shown to be the predominant pathway during sulfur deprivation (Antal et al., 2003; Fouchard et al., 2005). The indirect pathway consists of a two-step process, in which reduced equivalents stored as starch during the aerobic phase are reinjected during the anaerobic phase into the photosynthetic electron transport chain downstream of PSII. Activity of the indirect pathway in H$_2$ production can be estimated by inhibiting residual PSII activity using DCMU (Fouchard et al., 2005; Chochois et al., 2009). Based on such a measurement, the contribution of the indirect pathway to H$_2$ production has been reported to be variable, depending on experimental conditions and particularly on the phase of the sulfur deprivation process (Kosourov et al., 2003; Laurinavichene et al., 2004; Fouchard et al., 2005). In our conditions, activity of the indirect pathway was about 10 times lower than that of the direct pathway under

conditions of sulfur deficiency (Chochois et al., 2009). We observed that in the presence of DCMU (as in its absence), the H$_2$ production rate measured in the *pgrl1* mutant was strongly increased compared with that measured in the wild type (see Supplemental Figure 4 online). Hydrogenase activity measurements were then performed in the wild type and *pgrl1* strain by following H/D isotope exchange (Cournac et al., 2004). Upon anaerobic induction, similar hydrogenase exchange activity levels were measured in the wild type and in the *pgrl1* mutant (see Supplemental Table 1 online). We therefore conclude that differences in H$_2$ production rates do not result from changes in hydrogenase activity, but rather arise from differences in the rate of electron supply to the hydrogenase.
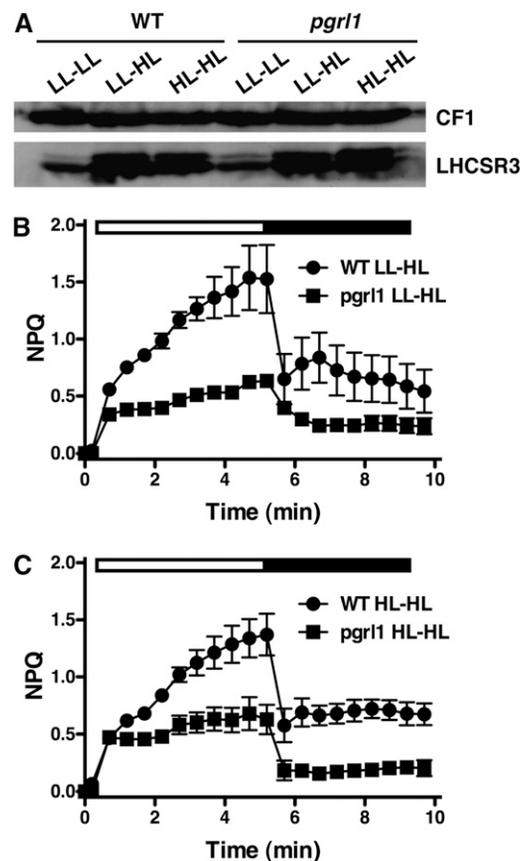
Figure 3. LHCSR3 Amounts and NPQ in Low Light and High Light Acclimated Cells.

Wild-type (WT) and *pgrl1* cells were adapted for 16 h in low light (LL; 20 μmol photons·m^{-2}·s^{-1}) or high light (HL; 200 μmol photons·m^{-2}·s^{-1}) in TAP medium and then shifted to HSM medium in LL or HL (LL-LL, LL-HL, and HL-HL culture) at an equal chlorophyll concentration (3.5 μgmL^{-1}).
(A) After 2 h, whole-cell extracts (2.5 μg chlorophyll) were fractionated on a 13% SDS-PAGE gel, and LHCSR3 levels were quantified by immunoblotting using CF1 (ATPase subunit) as loading control.
(B) and **(C)** Samples from the experiment described above were dark-adapted for 20 min, and NPQ was recorded during 5.2 min of illumination at 800 μmol photons m^{-2}·s^{-1} (white bar) followed by 4.3 min of darkness (black bar). Plotted values are the means of three measurements ± SD.
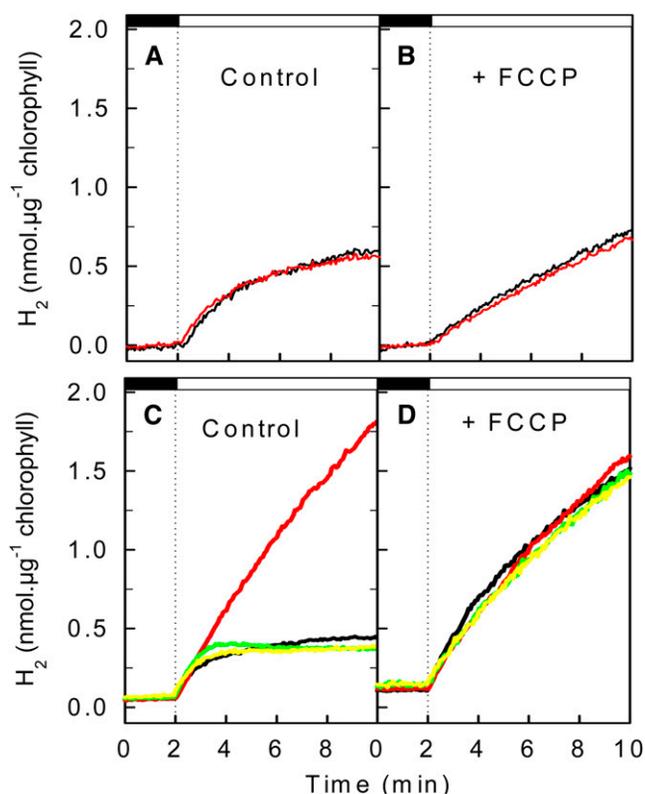
Figure 4. Short-Term Hydrogen Photoproduction under Anaerobiosis.

Hydrogen production was measured using a membrane inlet mass spectrometer. After induction of hydrogenase for 45 min in the dark under anaerobic conditions obtained by addition of glucose and glucose oxidase to the reaction medium, light was switched on (dashed line) either at 50 μmol photons·m^{-2}·s^{-1} PAR (**[A]** and **[B]**) or at 200 μmol photons·m^{-2}·s^{-1} (**[C]** and **[D]**). Hydrogen evolution was measured in the wild type (black line), in *pgrl1* (red line), and in the two complemented lines *pgrl1*::*PGRL1* 1 (green line) and *pgrl1*::*PGRL1* 2 (yellow line).
(A) and **(C)** Control experiments.
(B) and **(D)** Effect of the uncoupling agent FCCP added at a final concentration of 2 μM 3 min before the start of the experiment.

Since starch has been reported to fuel both pathways of H$_2$ production, we analyzed intracellular starch during sulfur deprivation experiments (Figure 6). Whereas no difference was observed during the starch accumulation phase, starch degradation was faster in the *pgrl1* mutant under conditions where the direct pathway prevails (Figure 6A). On the other hand, starch was consumed in a similar manner in the wild type and *pgrl1* under conditions where the indirect pathway prevails (Figure 6B).

Immunoblot analysis of key proteins was then performed during sulfur deprivation in wild-type cells, in the *pgrl1* knockout mutant (*pgrl1-ko*), and in *pgrl1-kd*, a previously described knock-down *pgrl1* line (Petroutsos et al., 2009). COX2B, a typical marker for respiratory electron protein complexes, was more abundant in both *pgrl1-kd* and *pgrl1-ko* cells (Figure 7). This confirms previously published findings showing increased abundance of COX2B and increased respiration in *pgrl1-kd* cells (Petroutsos

et al., 2009). In *pgrl1-ko* cells, LHCA3 levels were below the detection level. This is in line with our finding that in *pgrl1-kd* cells the amount of LHCA3 is decreased compared with wild-type cells (Petroutsos et al., 2009). N-terminal processing of LHCA3, a key mechanistic event in the remodeling process of PSI and its associated light-harvesting proteins (LHCI), is induced by iron deficiency in *Chlamydomonas* and correlates with a functional drop in excitation energy transfer efficiency between LHCI and PSI (Naumann et al., 2005). It is of note that the *pgrl1-ko* cells displayed an iron-deficient phenotype as previously described for the *pgrl1-kd* mutant strain (Petroutsos et al., 2009). Specifically, *pgrl1-ko* cells grown at 0.5 μM Fe show much higher induction of iron assimilation components (iron assimilatory protein FEA1 and ferroxidase FOX1) and more severe degradation of ferredoxin and of LHCA3 at 0.5 and 1 μM Fe compared with the wild-type cells grown at the same Fe concentrations. Interestingly, the level of LHCSR3 was highly decreased in response to PGRL1 depletion or reduction in *C. reinhardtii* mutants under sulfur deficiency (Figure 7), indicating that PGRL1 function is required for proper adaptation to low sulfur availability.

DISCUSSION

From the screening of a *Chlamydomonas* insertion mutant library based on the analysis of chlorophyll fluorescence transients of single algal colonies, we isolated a knockout mutant of
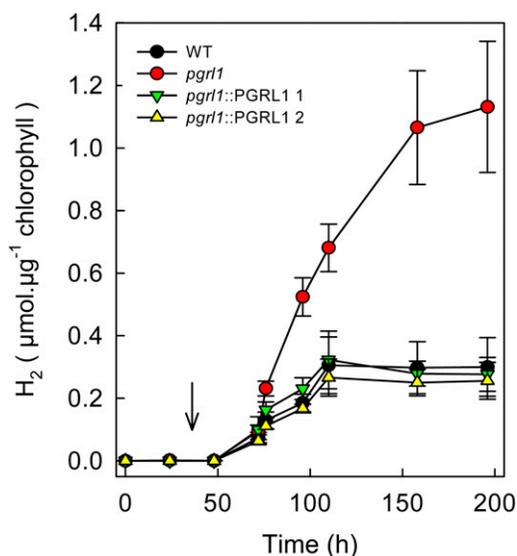
Figure 5. Long-Term Hydrogen Production Measured in Response to Sulfur Deficiency.

Exponentially growing cells (TAP medium) were centrifuged and resuspended in a sulfur-free medium (initial cellular concentration was 4×10^6 cells·mL^{-1}) in illuminated (200 μmol photons·m^{-2}·s^{-1}) sealed flasks. When indicated by an arrow, the cell suspension was bubbled with N$_2$ to remove residual O$_2$ and synchronize hydrogen production. Data are expressed as the average values ± SD of three independent experiments. WT, wild type.
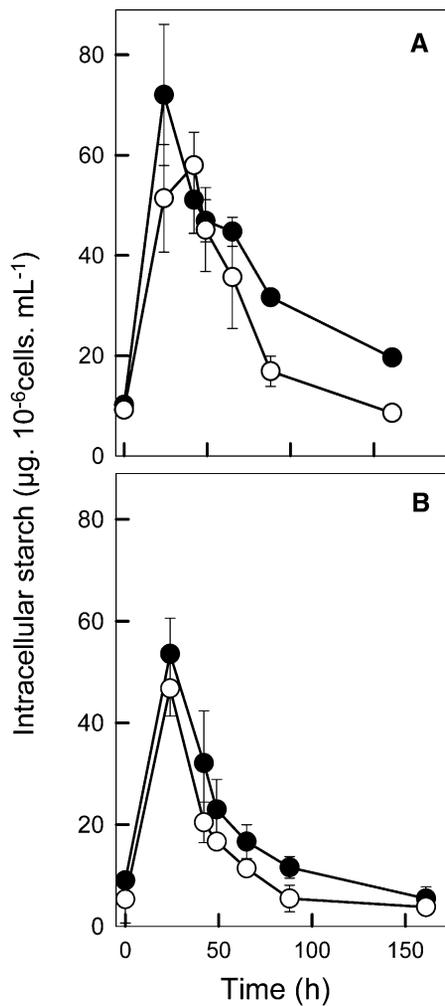
Figure 6. Intracellular Starch Contents Measured during Long-Term Hydrogen Photoproduction under Conditions of Sulfur Deprivation.

Wild-type (closed circle); *pgrl1* (open circle). Data are expressed as the average value ± SD (bars) of three independent experiments. Starch accumulated during the first 24 h of sulfur deprivation and was then progressively degraded.

(A) Control in the absence of DMCU (similar experiment as in Figure 5).
(B) In the presence of DCMU (20 μM final concentration) added at *t* = 24 h (similar experiment as in Supplemental Figure 4 online).

the *PGRL1* gene. As previously reported in *Arabidopsis pgr5* (Munekage et al., 2002) and *pgrl1* mutants (DalCorso et al., 2008), the *Chlamydomonas pgrl1* mutant shows reduced activities of both NPQ (Figures 1 to 3) and CEF (Table 1). In *Arabidopsis* mutants, the NPQ decrease was attributed to a deficiency in CEF resulting in the establishment of a lower *trans*-thylakoidal proton gradient (Munekage et al., 2002; DalCorso et al., 2008). Indeed, PGRL1 has been identified as an essential component of CEF in interaction with PGR5 (DalCorso et al., 2008). Since LHCSR3 accumulation occurs in a similar manner in response to high light both in the wild type and *pgrl1*, the decreased activity of NPQ observed in the mutant likely results from a decrease in the CEF-dependent *trans*-thylakoidal proton gradient.

When *Chlamydomonas* cells are adapted to anaerobic conditions, the plastidial hydrogenase is induced resulting in photoproduction of hydrogen (Melis and Happe, 2001). This phenomenon is strongly stimulated in the *pgrl1* mutant both in short-term experiments, where anaerobiosis is maintained by addition of glucose and glucose oxidase, and in long-term experiments in conditions of sulfur deprivation (Figures 4 and 5). Under anaerobic conditions, activity of CEF was increased in the wild type but not in *pgrl1* (Table 1). Such a stimulation of CEF under anaerobiosis is related to the phenomenon of state transition (Finazzi et al., 2002). During this process, the increased redox state of the PQ pool activates the *stt7* kinase (Depège et al., 2003), resulting in the migration of phosphorylated LHCII from PSII to PSI and in a switch from state 1 to state 2 (Wollman and Delepelaire, 1984). A supercomplex between PSI-LHCI-LHCII-FNR-cytochrome b_6/f and PGRL1 is formed in state 2, allowing efficient operation of CEF around PSI (Iwai et al., 2010). Thus, anaerobiosis is particularly favorable to the establishment of a strong CEF activity (Table 1), explaining why knockout of the *PGRL1* gene confers a strong phenotype in these conditions. In addition, the uncoupling agent FCCP, which suppresses the *trans*-membrane proton gradient, increased hydrogen photoproduction in the wild type up to a level similar to that measured in *pgrl1* (Figure 4). We therefore conclude that under anaerobic conditions, the proton gradient generated by CEF exerts a limitation on the electron supply to the hydrogenase. Because this effect is observed both in conditions where PSII (direct pathway) or starch breakdown (indirect pathway) feed the photosynthetic electron transport chain, we conclude that the control point of electron transport is located at a common step between these two pathways (i.e., downstream of the PQ pool). A strong control of linear electron flow by the *trans*-thylakoidal proton gradient has been previously reported to exist in land plant chloroplasts at the level of plastoquinol oxidation by the cytochrome b_6/f complex (Genty and Harbinson, 1996; Kramer et al., 1999). Under normal operation of photosynthesis, the pH of the lumen is maintained at levels that do not inhibit cytochrome b_6/f activity. However, when some disequilibrium occurs between the light supply and the metabolic demand (e.g., induction of photosynthesis, high light and low CO_2, low temperature stress, etc.), modulation of cytochrome b_6/f activity by the proton gradient would prevent overacidification of the thylakoid lumen. Recently, the existence of a strong effect of the lumen pH on cytochrome b_6/f activity was reported in transgenic tobacco lines expressing reduced ATPase levels (Rott et al., 2011).

Under aerobic conditions, a transient increase in ETR was observed in *pgrl1* in comparison to the wild type during a dark-to-light transient following dark adaptation (Figure 1F). This increase, which was enhanced at a higher light intensity (see Supplemental Figure 5 online), likely results from a downregulation of photosynthetic electron flow in wild-type cells during the induction phase of photosynthesis. Indeed, under conditions where photosynthesis is not fully operational due to inactivation of Calvin cycle enzymes (following dark adaptation), the proton gradient cannot be efficiently dissipated by the action of ATPase (which is deactivated in the dark). Under these conditions, the proton gradient generated by activity of CEF would be sufficient to generate a downregulation of the photosynthetic electron
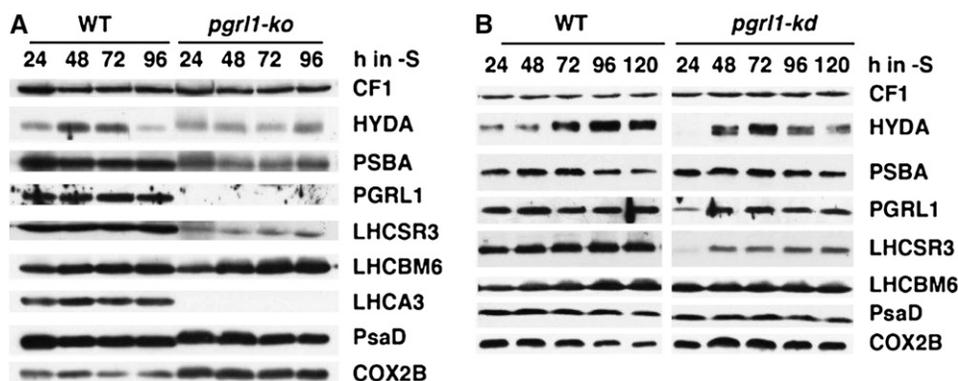
Figure 7. Immunoblot Analysis of Key Proteins during Sulfur Deprivation in the Wild Type, in a *pgrl1* Knockdown Line (*pgrl1-kd*), and in the *pgrl1* Knockout Mutant (*pgrl1-ko*) during Sulfur Deprivation.

Extracts were prepared from two independent sulfur deprivation experiments and fractionated on 13% SDS-PAGE, and the abundance of CF1, HYDA, PSBA, PGRL1, LHCSR3, LHCBM6, LHCA3, PSAD, and COX2B was analyzed by immunoblotting. CF1 (ATPase) signal served as a loading control.
(A) Whole-cell extracts of the wild type (WT) and *pgrl1-ko* (*i-e pgrl1*). All immunoblots originate from SDS-PAGE gels loaded with 2.5 µg chlorophyll per lane.
(B) Whole-cell extracts of the wild type and *pgrl1-kd*. All immunoblots originate from SDS-PAGE gels loaded with 40 µg protein per lane, with the exception of the HYDA immunoblot, whose gel was loaded with 3 µg chlorophyll per lane.

transport in the wild type, which would be released in the CEF-deficient mutant.

In contrast with *Arabidopsis pgr5* and *pgrl1* mutants, in which photosynthetic activity is severely affected under high light (Munekage et al., 2002; DalCorso et al., 2008), photosynthesis is not reduced in *Chlamydomonas pgrl1* (Figure 2D). This indicates that compensatory mechanisms allowing an efficient dissipation of excess reducing power are probably more active in microalgae than in land plants, therefore avoiding the irreversible PSI inactivation observed in the *Arabidopsis* mutants (Munekage et al., 2002, 2008). The increased mitochondrial activity and COX expression (Figure 7) observed in *pgrl1* knockdown lines (Petroutsos et al., 2009) likely reflects an increased cooperation between photosynthesis and mitochondrial respiration. Such cooperation has been previously documented in a *Chlamydomonas* mutant that is deficient in plastidial ATPase but able to restore photoautotrophic growth thanks to an increased cooperation between chloroplasts and mitochondria (Lemaire et al., 1988). This phenomenon, which requires efficient export of reducing power from chloroplasts to mitochondria, for instance, using the malate/oxalo-acetate shuttle, has been reported to be enhanced in the *Arabidopsis pgr5* mutant, particularly under high light (Yoshida et al., 2007).

Both *pgr5* and *pgrl1* trancript levels are upregulated under iron deficiency in *C. reinhardtii.* For PGRL1, this increased expression has been also demonstrated at the protein level (Petroutsos et al., 2009). Under anaerobic growth conditions, PGRL1 is not increased in its expression compared with aerobic conditions (Terashima et al., 2010), although CEF is induced. Thus, it is likely that regulation of CEF via PGRL1 is not facilitated by altering the amounts of PGRL1. Such a regulation could be mediated via the redox and/or the iron binding state of PGRL1 as previously suggested (Petroutsos et al., 2009).

We therefore interpret our results as follows. Under conditions where the ATP demand by photosynthesis is low (such as during

induction of photosynthesis or during anaerobiosis, sulfur or iron deprivation, etc.) the proton gradient is not efficiently dissipated, resulting in a limitation of the electron transport at cytochrome b_6/f in wild-type cells. Photosynthetic electron flow is not restricted in *pgrl* due to a lower *trans*-thylakoidal pH gradient resulting from a lower CEF activity. Under aerobiosis, excess reducing power would be redirected to the mitochondria. Under anaerobiosis, electrons would be directed toward the hydrogenase operating as a safety valve (Happe and Kaminski, 2002; Hemschemeier et al., 2009).

Previous reports have postulated the existence of a relationship between hydrogen photoproduction and CEF (Kruse et al., 2005b; Antal et al., 2009). A *Chlamydomonas* mutant (*stm6*) affected in a nuclear gene (*MOC1*) encoding a mitochondrial protein was shown to produce higher amounts of hydrogen (5 times more) than the wild-type strain (Kruse et al., 2005b). Although this mutant is affected in the assembly of the mitochondrial respiratory chain (Schönfeld et al., 2004), it was concluded that the stimulation of hydrogen production results from a defect in CEF around PSI in *stm6* (Kruse et al., 2005b). More recently, and in line with our data, Antal et al. (2009) reported a stimulatory effect of uncouplers and antimycin A, an inhibitor of ferredoxin-quinone-reductase–mediated CEF, on hydrogen photoproduction in *Chlamydomonas*. The authors proposed that ferredoxin-quinone-reductase–dependent CEF slows down hydrogen photoproduction more than 2-fold (Antal et al., 2009).

Hydrogenases have been found as activities or genes in several eukaryotic microalgae species, including chlorophyceae, prasinophyceae, trebouxiaceae, and diatoms (Peltier et al., 2010). Although H_2 photoproduction is a wasteful energy process, hydrogenases have been suggested to confer a selective advantage under anaerobiosis, by avoiding overreduction of PSI electron acceptors (Happe et al., 2002; Hemschemeier et al., 2009). We propose here that H_2 photoproduction could be

viewed as a key player in an energy conserving mechanism. Indeed, electron flow toward the hydrogenase would result in ATP production in two different ways: (1) by directly generating a proton gradient, and (2) by setting an adequate redox poise of PSI electron acceptors, which triggers the establishment of PGRL1-mediated CEF, thus likely conferring a selective advantage under anaerobic environments. At a biotechnological level, the modulation of the *trans*-thylakoidal proton gradient by PGRL1 expression opens new perspectives in the reprogramming of microalgae bioenergetics toward improved H_2 photoproduction.

METHODS

Strains and Mutant Screen

The *Chlamydomonas reinhardtii* wild-type strain 137c (*mt⁻ nit1 nit2*) was grown at 25°C in TAP liquid medium under continuous illumination (40 μmol photons·m^{-2}·s^{-1}). Photoautotrophic cultures were performed using a minimal medium (Harris, 1989). Mutants were generated by random insertion of the *Aph*VIII cassette conferring paromomycin resistance (Chochois et al., 2010). After selection on solid minimal medium supplemented with paromomycin (10 μg·mL^{-1}), insertion mutants were screened for abnormal chlorophyll fluorescence transients recorded during a 30 μmol photons·m^{-2}·s^{-1} illumination (465-nm LEDs filtered with a Schott BG39 glass filter) by imaging fluorescence emission (above 700 nm using a Kodak Wratten 70 filter) using a cooled CCD camera. A homemade imaging application (Labview; National Instruments) was developed to analyze fluorescence transients of all single colonies. The *pgrl1* knockout mutant (*pgrl1-ko*) was isolated from the present mutant screen. Isolation of the *pgrl1* knockdown line (*pgrl1-kd*), a *Chlamydomonas* RNA interference line expressing a lower level of PGRL1, has been previously described (Petroutsos et al., 2009).

Absorption Change Measurements

P700 absorption change kinetics and carotenoid electrochromic bandshifts were measured using a JTS 10 spectrophotometer equipped with light emitting diodes (BioLogic). P700 measurements were performed at 705 nm as described previously (Alric et al., 2010). Electrochromic carotenoid bandshift measurements were performed at 520 nm (Witt, 1979; Joliot and Joliot, 2002). For both measurements, PSII activity was blocked by addition of DCMU (final concentration 10 μM) and hydroxylamine (final concentration 1 mM). Short (6 ns) laser pulses (provided by a Nd:YAG pumping a dye cell filled with 4-dicyanomethylene-2-methyl-6-p-dimethylaminostyryl-4H-pyran) were used as single turnover flashes.

Chlorophyll fluorescence measurements were performed using a Dual Pam-100 (Heinz Walz). Samples were placed into a cuvette under constant stirring at room temperature (23°C). In a first set of experiments, cells were dark-adapted (30 min) and chlorophyll fluorescence was recorded, saturating flashes being given at different time points during a transition from darkness to 75 μmol photons·m^{-2}·s^{-1} light. In a second set of experiments, cells were not dark-adapted. Actinic light was increased stepwise from 3 to 960 μmol photons·m^{-2}·s^{-1}; after 40 s under each given light regime, a saturating flash (10,000 μmol photons·m^{-2}·s^{-1}, 200-ms duration) was supplied to measure Fm'. NPQ and ETR were calculated as described previously (Rumeau et al., 2005).

Genomic DNA Analysis

Total DNA was prepared from 5·10^7 *Chlamydomonas* cells. Cell pellets were resuspended in 500 μL lysis buffer (100 mM Tris-HCl, pH 8.0, 1.75 mM EDTA, and 3% [w/v] SDS). After addition of 6 μL proteinase K (20 mg·mL^{-1}), lysates were incubated for 2 h at 55°C, and 80 μL of 5 M KCl, then 70 μL of a 10% CTAB solution (hexadecyl-trimethylammoniumbromide; Sigma-Aldrich) in 0.7 M NaCl were further added. Samples were then incubated for 10 min at 65°C. After two phenol-chloroform extractions and a final chloroform extraction, the nucleic acids were precipitated by addition of 600 μL propan-2-ol, recovered by a 15 min centrifugation, washed with 70% ethanol, dried, and resuspended in 50 μL sterile water. For recovery and mapping of genomic sequences flanking the cassette insertion site, thermal asymmetric interlaced PCR was used as described by Liu et al. (1995). Thermal asymmetric interlaced PCR was performed using three nested specific primers designed from the *AphVIII* cassette sequence (5′-ACCGGCACTCCGATCTCGCG-3′, Tm = 69.5°C; 5′-GCGAGCTGGCCCACGAGGAG-3′, Tm = 69.3°C; and 5′-TCGGGCCGGAGTGTTCCGCG-3′, Tm = 73.8°C) in successive reactions together with a shorter arbitrary degenerate primer (5′-STAGASTSTSGWGTS-3′, 64-fold degeneracy, average Tm = 47.9°C; 5′-WCTSGASTSANCATC-3′, 128-fold degeneracy, average Tm = 46.6°C; and 5′-SASCASASTSWWCTS-3′, 256-fold degeneracy, average Tm = 47.9°C) so that the relative amplification efficiencies of specific and nonspecific products could be thermally controlled. The position of the *AphVIII* insertion was confirmed by sequencing the entire *PGRL1* gene in the *pgrl1* mutant amplified by PCR according to Liu et al. (1995) and using the following primers: 5′-ATGCAGACCACCGTGCTCCGTTCTTCC-3′ and 5′- TTACGCAGCGGCCTTAGCCTTCTTCTTGGC-3′ designed from the *PGRL1* gene sequence (JGIv4.0).

RNA Analysis

Total RNA was isolated using TRIzol (Life Technologies). RT-PCR was performed on 1 μg of the total RNA using the SuperScript III One-Step RT-PCR system kit (Life Technologies). Specific primers were selected for a β-tubulin (*tub1* protein ID 129876) (5′-GCCCTGTACGACATCTGCTT-3′ and 5′-GCTGATCAGGTGGTTCAGGT-3′) and *pgrl1* (5′- ATGCAGACCA-CCGTGCTCCGTTCTTCC-3′ and 5′-TTACGCAGCGGCCTTAGCCTTCT-TCTTGGC-3′).

Immunoblot Analysis

Cells were lysed by sonication in a pH 7.5 200 mM HEPES buffer containing 150 mM NaCl and a protease inhibitor cocktail for plant cells (P8849 Sigma-Aldrich). SDS (1.5% final concentration) was added before precipitation in acetone 80%. The protein pellet was resuspended in denaturing blue NuPage (Invitrogen). About 10 μg of proteins were loaded on 13% SDS-PAGE gels and transferred to nitrocellulose membrane using a semidry transfer technique when not specified otherwise. Immunodetection was performed using antibodies raised against PSAD (Naumann et al., 2005), LHCSR3 (Naumann et al., 2007), LHCA3 (Moseley et al., 2002), LHCBM6 (Hippler et al., 2001), PGRL1 (Naumann et al., 2007), and CF1 (Moseley et al., 2002). PSBA and COX2B antibodies were obtained from Agrisera, and HYDA antibody was a kind gift from Peter J. Nixon (Imperial College, London). A protein gel blotting kit (Roche) was used with anti-rabbit peroxidase-conjugated antibodies. A specific polyclonal antibody was raised against a poly His-tagged recombinant PGRL1 protein. A fragment of the gene encoding middle part of the PGRL1 protein was cloned in the *Escherichia coli* expression vector pQE60 (Qiagen). The DNA fragment was amplified with the primers PGRL1pQE30F (5′-GGCC*GGATCC*TCGGCGAAGA-AGGACGATGG-3′; Tm = 70°C) and PGRL1pQE60R (5′-GGCC*AGATC-T*AGGCTCGGCATCGGCATAC-3′; Tm = 67°C) (in italics are the added restriction sites for *Bam*HI and *Bgl*II, respectively). The PCR was performed with Phusion High-Fidelity PCR master mix (Finnzymes). The resulting plasmid was used to transform the *E. coli* strain M15pREP4 for the production of His-tagged PGRL1 fragment. Upon induction by

isopropyl β-D-1-thiogalactopyranoside, the His-tagged PGRL1 protein was purified using a fast protein liquid chromatography system equipped with a His Trap HP column (GE Healthcare). The PGRL1 antibody raised in rabbit was used at a 1:4000 dilution. Relative quantification of PGRL1 was achieved in the complemented lines using a calibration curve obtained by serial 4-fold dilutions of wild-type extracts. Images were captured using G:BOX Chemin XL (Syngene) followed by analysis of band intensity using GeneTools software (Syngene).

Complementation of *pgrl1*

A genomic clone of *PGRL1* with its own promoter (~1100 bp upstream the 5′-untranslated region) was amplified by high fidelity TAQ polymerase (Herculase Stratagène) from wild-type genomic DNA using the primers 5′-TGTGGCGCTATCGCTCAGTA-3′ and 5′-GAATCCCGGGATTCATGT-CACGCTCG-3′ and cloned into a pSL-hyg vector carrying hygromycin resistance (Berthold et al., 2002). Transformed cells were selected on 10 μM hygromycin and then screened for PGRL1 protein levels by immunodetection. Two partially complemented lines, expressing around 50 to 60% of the wild-type PGRL1 level, were selected for further experimentation.

Measurement of H$_2$ Photoproduction

Short-term rates of H$_2$ production were determined using a water-jacketed thermoregulated (25°C) reaction vessel (1.5 mL) coupled to a mass spectrometer (model Prima δB; Thermo Electron) through a membrane inlet system. The cell suspension (~25 μg of chlorophyll per mL) was placed in the reaction vessel, and glucose (20 mM final concentration), glucose oxidase (10 units), and 5000 units catalase were added to reach and further maintain anoxia. After a 45-min induction period in the dark, the suspension was illuminated at light intensities of 200 or 50 μmol photons·m^{-2}·s^{-1}. In some experiments, FCCP (2 μM final concentration) was added 3 min before illumination. O$_2$, H$_2$, and CO$_2$ were monitored simultaneously and gas exchange rates determined as described previously (Cournac et al., 2002). Long-term H$_2$ photoproduction was measured in the *pgrl1* knockout mutant under conditions of sulfur deficiency (Chochois et al., 2009). Cells were grown in TAP medium until reaching 6·10^6 cells·mL^{-1} and then washed twice and resuspended in a S-deprived medium at t$_0$ in sealed 250-mL glass flasks (Schott). Cultures were placed under continuous illumination (200 μmol photons·m^{-2}·s^{-1}) with constant stirring at room temperature (25°C). In some experiments, DCMU was added (20 μM final concentration) to the cell suspension at 24 h. To ensure that anoxia was reached simultaneously in the different flasks, all flasks were bubbled with N$_2$ for 6 min either 46 h after t$_0$ (or after 24 h in the case of DCMU experiments). H$_2$ and O$_2$ concentrations of the gas phase were analyzed from a 0.5-mL gas sample at different time intervals using a mass spectrometer (Prisma QMS 200; Pfeiffer Vacuum).

Accession Number

Sequence data from this article can be found in the Phytozome database under accession number Cre07.g340200 (*PGRL1*).

Supplemental Data

The following materials are available in the online version of this article.

Supplemental Figure 1. Time Course of Chlorophyll Fluorescence during a Dark–Light Transient in *pgrl1* and Wild-Type Cells.

Supplemental Figure 2. Flash-Induced Absorption Change Measurements Used to Determine Activity of Cyclic Electron Flow around PSI.

Supplemental Figure 3. Long-Term Hydrogen Photoproduction in Conditions of Sulfur Deficiency.

Supplemental Figure 4. Long-Term Hydrogen Production under Sulfur Deficiency Measured in the Presence of DCMU (Indirect Pathway).

Supplemental Figure 5. Time Course of Chlorophyll Fluorescence, ETR, and NPQ during a Dark–Light Transient in *pgrl1* and Wild-Type Cells.

Supplemental Table 1. Measurement of Hydrogenase Activity by H/D Isotope Exchange in Wild-Type and *pgrl1* Cells Following Hydrogenase Induction in Anaerobic Conditions.

AUTHOR CONTRIBUTIONS

L.C., M.H., and G.P. designed the experiments. I.M.R. and B. Genty designed the mutant screening device. B. Ghysels, D.T., J.A., J.P., J.-M.A., S.C., P.A., D.P., I.T., D.K., and A.B. performed experiments. B. Ghysels, B. Genty, D.T., J.A., L.C., T.H., M.H., and G.P. discussed and interpreted the data. G.P. wrote the article.

REFERENCES

Alric, J., Lavergne, J., and Rappaport, F. (2010). Redox and ATP control of photosynthetic cyclic electron flow in *Chlamydomonas reinhardtii* (I) aerobic conditions. Biochim. Biophys. Acta **1797:** 44–51.

Antal, T.K., Krendeleva, T.E., Laurinavichene, T.V., Makarova, V.V., Ghirardi, M.L., Rubin, A.B., Tsygankov, A.A., and Seibert, M. (2003). The dependence of algal H$_2$ production on Photosystem II and O$_2$ consumption activities in sulfur-deprived *Chlamydomonas reinhardtii* cells. Biochim. Biophys. Acta **1607:** 153–160.

Antal, T.K., Volgusheva, A.A., Kukarskih, G.P., Krendeleva, T.E., and Rubin, A.B. (2009). Relationships between H$_2$ photoproduction and different electron transport pathways in sulfur-deprived *Chlamydomonas reinhardtii.* Int. J. Hydrogen Energy **34:** 9087–9094.

Berthold, P., Schmitt, R., and Mages, W. (2002). An engineered *Streptomyces hygroscopicus aph 7″* gene mediates dominant resistance against hygromycin B in *Chlamydomonas reinhardtii.* Protist **153:** 401–412.

Chochois, V., Constans, L., Dauvillée, D., Beyly, A., Solivérès, M., Ball, S., Peltier, G., and Cournac, L. (2010). Relationships between PSII-independent hydrogen bioproduction and starch metabolism as

evidenced from isolation of starch catabolism mutants in the green alga *Chlamydomonas reinhardtii.* Int. J. Hydrogen Energy **35:** 10731–10740.

Chochois, V., Dauvillée, D., Beyly, A., Tolleter, D., Cuiné, S., Timpano, H., Ball, S., Cournac, L., and Peltier, G. (2009). Hydrogen production in *Chlamydomonas*: Photosystem II-dependent and -independent pathways differ in their requirement for starch metabolism. Plant Physiol. **151:** 631–640.

Cournac, L., Guedeney, G., Peltier, G., and Vignais, P.M. (2004). Sustained photoevolution of molecular hydrogen in a mutant of *Synechocystis* sp. strain PCC 6803 deficient in the type I NADPH-dehydrogenase complex. J. Bacteriol. **186:** 1737–1746.

Cournac, L., Mus, F., Bernard, L., Guedeney, G., Vignais, P., and Peltier, G. (2002). Limiting steps of hydrogen production in *Chlamydomonas reinhardtii* and *Synechocystis* PCC 6803 as analysed by light-induced gas exchange transients. Int. J. Hydrogen Energy **27:** 1229–1237.

DalCorso, G., Pesaresi, P., Masiero, S., Aseeva, E., Schünemann, D., Finazzi, G., Joliot, P., Barbato, R., and Leister, D. (2008). A complex containing PGRL1 and PGR5 is involved in the switch between linear and cyclic electron flow in *Arabidopsis.* Cell **132:** 273–285.

Dementin, S., et al. (2009). Introduction of methionines in the gas channel makes [NiFe] hydrogenase aero-tolerant. J. Am. Chem. Soc. **131:** 10156–10164.

Depège, N., Bellafiore, S., and Rochaix, J.D. (2003). Role of chloroplast protein kinase Stt7 in LHCII phosphorylation and state transition in *Chlamydomonas.* Science **299:** 1572–1575.

Desplats, C., Mus, F., Cuiné, S., Billon, E., Cournac, L., and Peltier, G. (2009). Characterization of Nda2, a plastoquinone-reducing type II NAD(P)H dehydrogenase in *Chlamydomonas* chloroplasts. J. Biol. Chem. **284:** 4148–4157.

Finazzi, G., Rappaport, F., Furia, A., Fleischmann, M., Rochaix, J.D., Zito, F., and Forti, G. (2002). Involvement of state transitions in the switch between linear and cyclic electron flow in *Chlamydomonas reinhardtii.* EMBO Rep. **3:** 280–285.

Florin, L., Tsokoglou, A., and Happe, T. (2001). A novel type of iron hydrogenase in the green alga *Scenedesmus obliquus* is linked to the photosynthetic electron transport chain. J. Biol. Chem. **276:** 6125–6132.

Fouchard, S., Hemschemeier, A., Caruana, A., Pruvost, J., Legrand, J., Happe, T., Peltier, G., and Cournac, L. (2005). Autotrophic and mixotrophic hydrogen photoproduction in sulphur-deprived chlamydomonas cells. Appl. Environ. Microbiol. **71:** 6199–6205.

Gaffron, H., and Rubin, J. (1942). Fermentative and photochemical production of hydrogen in algae. J. Gen. Physiol. **26:** 219–240.

Genty, B., and Harbinson, J. (1996). Regulation of light utilization for photosynthetic electron transport. In Photosynthesis and the Environment, N.R. Baker, ed (Dordrecht, The Netherlands: Kluwer Academic Publishers), pp. 67–99.

Ghirardi, M.L., Zhang, L., Lee, J.W., Flynn, T., Seibert, M., Greenbaum, E., and Melis, A. (2000). Microalgae: a green source of renewable H(2). Trends Biotechnol. **18:** 506–511.

Happe, T., Hemschemeier, A., Winkler, M., and Kaminski, A. (2002). Hydrogenases in green algae: Do they save the algae's life and solve our energy problems? Trends Plant Sci. **7:** 246–250.

Happe, T., and Kaminski, A. (2002). Differential regulation of the Fe-hydrogenase during anaerobic adaptation in the green alga *Chlamydomonas reinhardtii.* Eur. J. Biochem. **269:** 1022–1032.

Harris, E.H. (1989). The *Chlamydomonas* Sourcebook: A Comprehensive Guide to Biology and Laboratory Use. (San Diego, CA: Academic Press).

Healey, F.P. (1970). Hydrogen evolution by several algae. Planta **91:** 220–226.

Hemschemeier, A., Melis, A., and Happe, T. (2009). Analytical approaches to photobiological hydrogen production in unicellular green algae. Photosynth. Res. **102:** 523–540.

Hippler, M., Klein, J., Fink, A., Allinger, T., and Hoerth, P. (2001). Towards functional proteomics of membrane protein complexes: Analysis of thylakoid membranes from *Chlamydomonas reinhardtii.* Plant J. **28:** 595–606.

Iwai, M., Takizawa, K., Tokutsu, R., Okamuro, A., Takahashi, Y., and Minagawa, J. (2010). Isolation of the elusive supercomplex that drives cyclic electron flow in photosynthesis. Nature **464:** 1210–1213.

Jans, F., Mignolet, E., Houyoux, P.A., Cardol, P., Ghysels, B., Cuiné, S., Cournac, L., Peltier, G., Remacle, C., and Franck, F. (2008). A type II NAD(P)H dehydrogenase mediates light-independent plastoquinone reduction in the chloroplast of *Chlamydomonas.* Proc. Natl. Acad. Sci. USA **105:** 20546–20551.

Joliot, P., and Joliot, A. (2002). Cyclic electron transfer in plant leaf. Proc. Natl. Acad. Sci. USA **99:** 10209–10214.

Joliot, P., and Joliot, A. (2008). Quantification of the electrochemical proton gradient and activation of ATP synthase in leaves. Biochim. Biophys. Acta **1777:** 676–683.

Kosourov, S., Seibert, M., and Ghirardi, M.L. (2003). Effects of extracellular pH on the metabolic pathways in sulfur-deprived, H$_2$-producing *Chlamydomonas reinhardtii* cultures. Plant Cell Physiol. **44:** 146–155.

Kramer, D.M., Sacksteder, C.A., and Cruz, J.A. (1999). How acidic is the lumen? Photosynth. Res. **60:** 151–163.

Kruse, O., Rupprecht, J., Bader, K.P., Thomas-Hall, S., Schenk, P.M., Finazzi, G., and Hankamer, B. (2005b). Improved photobiological H$_2$ production in engineered green algal cells. J. Biol. Chem. **280:** 34170–34177.

Kruse, O., Rupprecht, J., Mussgnug, J.H., Dismukes, G.C., and Hankamer, B. (2005a). Photosynthesis: A blueprint for solar energy capture and biohydrogen production technologies. Photochem. Photobiol. Sci. **4:** 957–970.

Laurinavichene, T., Tolstygina, I., and Tsygankov, A. (2004). The effect of light intensity on hydrogen production by sulfur-deprived *Chlamydomonas reinhardtii.* J. Biotechnol. **114:** 143–151.

Lemaire, C., Wollman, F.A., and Bennoun, P. (1988). Restoration of phototrophic growth in a mutant of *Chlamydomonas reinhardtii* in which the chloroplast *atpB* gene of the ATP synthase has a deletion: An example of mitochondria-dependent photosynthesis. Proc. Natl. Acad. Sci. USA **85:** 1344–1348.

Liu, Y.G., Mitsukawa, N., Oosumi, T., and Whittier, R.F. (1995). Efficient isolation and mapping of *Arabidopsis thaliana* T-DNA insert junctions by thermal asymmetric interlaced PCR. Plant J. **8:** 457–463.

Melis, A. (2002). Green alga hydrogen production: Progress, challenges and prospects. Int. J. Hydrogen Energy **27:** 1217–1228.

Melis, A., and Happe, T. (2001). Hydrogen production. Green algae as a source of energy. Plant Physiol. **127:** 740–748.

Melis, A., Zhang, L.P., Forestier, M., Ghirardi, M.L., and Seibert, M. (2000). Sustained photobiological hydrogen gas production upon reversible inactivation of oxygen evolution in the green alga *Chlamydomonas reinhardtii.* Plant Physiol. **122:** 127–136.

Moseley, J.L., Allinger, T., Herzog, S., Hoerth, P., Wehinger, E., Merchant, S., and Hippler, M. (2002). Adaptation to Fe-deficiency requires remodeling of the photosynthetic apparatus. EMBO J. **21:** 6709–6720.

Munekage, Y., Hojo, M., Meurer, J., Endo, T., Tasaka, M., and Shikanai, T. (2002). PGR5 is involved in cyclic electron flow around photosystem I and is essential for photoprotection in Arabidopsis. Cell **110:** 361–371.

Munekage, Y.N., Genty, B., and Peltier, G. (2008). Effect of PGR5 impairment on photosynthesis and growth in *Arabidopsis thaliana.* Plant Cell Physiol. **49:** 1688–1698.

Naumann, B., Busch, A., Allmer, J., Ostendorf, E., Zeller, M., Kirchhoff, H., and Hippler, M. (2007). Comparative quantitative proteomics to investigate the remodeling of bioenergetic pathways under iron deficiency in *Chlamydomonas reinhardtii*. Proteomics **7:** 3964–3979.

Naumann, B., Stauber, E.J., Busch, A., Sommer, F., and Hippler, M. (2005). N-terminal processing of Lhca3 Is a key step in remodeling of the photosystem I-light-harvesting complex under iron deficiency in *Chlamydomonas reinhardtii.* J. Biol. Chem. **280:** 20431–20441.

Peers, G., Truong, T.B., Ostendorf, E., Busch, A., Elrad, D., Grossman, A.R., Hippler, M., and Niyogi, K.K. (2009). An ancient light-harvesting protein is critical for the regulation of algal photosynthesis. Nature **462:** 518–521.

Peltier, G., Tolleter, D., Billon, E., and Cournac, L. (2010). Auxiliary electron transport pathways in chloroplasts of microalgae. Photosynth. Res. **106:** 19–31.

Petroutsos, D., Terauchi, A.M., Busch, A., Hirschmann, I., Merchant, S.S., Finazzi, G., and Hippler, M. (2009). PGRL1 participates in iron-induced remodeling of the photosynthetic apparatus and in energy metabolism in *Chlamydomonas reinhardtii.* J. Biol. Chem. **284:** 32770–32781.

Rott, M., Martins, N.F., Thiele, W., Lein, W., Bock, R., Kramer, D.M., and Schöttler, M.A. (2011). ATP synthase repression in tobacco restricts photosynthetic electron transport, CO_2 assimilation, and plant growth by overacidification of the thylakoid lumen. Plant Cell **23:** 304–321.

Rumeau, D., Bécuwe-Linka, N., Beyly, A., Louwagie, M., Garin, J., and Peltier, G. (2005). New subunits NDH-M, -N, and -O, encoded by nuclear genes, are essential for plastid Ndh complex functioning in higher plants. Plant Cell **17:** 219–232.

Schönfeld, C., Wobbe, L., Borgstädt, R., Kienast, A., Nixon, P.J., and Kruse, O. (2004). The nucleus-encoded protein MOC1 is essential for mitochondrial light acclimation in *Chlamydomonas reinhardtii.* J. Biol. Chem. **279:** 50366–50374.

Stripp, S.T., Goldet, G., Brandmayr, C., Sanganas, O., Vincent, K.A., Haumann, M., Armstrong, F.A., and Happe, T. (2009). How oxygen attacks [FeFe] hydrogenases from photosynthetic organisms. Proc. Natl. Acad. Sci. USA **106:** 17331–17336.

Terashima, M., Specht, M., Naumann, B., and Hippler, M. (2010). Characterizing the anaerobic response of *Chlamydomonas reinhardtii* by quantitative proteomics. Mol. Cell. Proteomics **9:** 1514–1532.

Witt, H.T. (1979). Energy conversion in the functional membrane of photosynthesis. Analysis by light pulse and electric pulse methods. The central role of the electric field. Biochim. Biophys. Acta **505:** 355–427.

Wollman, F.A., and Delepelaire, P. (1984). Correlation between changes in light energy distribution and changes in thylakoid membrane polypeptide phosphorylation in *Chlamydomonas reinhardtii.* J. Cell Biol. **98:** 1–7.

Yoshida, K., Terashima, I., and Noguchi, K. (2007). Up-regulation of mitochondrial alternative oxidase concomitant with chloroplast over-reduction by excess light. Plant Cell Physiol. **48:** 606–614.

Control of Hydrogen Photoproduction by the Proton Gradient Generated by Cyclic Electron Flow in *Chlamydomonas reinhardtii*

Dimitri Tolleter, Bart Ghysels, Jean Alric, Dimitris Petroutsos, Irina Tolstygina, Danuta Krawietz, Thomas Happe, Pascaline Auroy, Jean-Marc Adriano, Audrey Beyly, Stéphan Cuiné, Julie Plet, Ilja M. Reiter, Bernard Genty, Laurent Cournac, Michael Hippler and Gilles Peltier

This information is current as of October 19, 2011

Supplemental Data	**http://www.plantcell.org/content/suppl/2011/07/15/tpc.111.086876.DC1.html**
References	This article cites 52 articles, 24 of which can be accessed free at: http://www.plantcell.org/content/23/7/2619.full.html#ref-list-1
Permissions	https://www.copyright.com/ccc/openurl.do?sid=pd_hw1532298X&issn=1532298X&WT.mc_id=pd_hw1532298X
eTOCs	Sign up for eTOCs at: http://www.plantcell.org/cgi/alerts/ctmain
CiteTrack Alerts	Sign up for CiteTrack Alerts at: http://www.plantcell.org/cgi/alerts/ctmain
Subscription Information	Subscription Information for *The Plant Cell* and *Plant Physiology* is available at: http://www.aspb.org/publications/subscriptions.cfm